

Little change in global drought over the past 60 years

Justin Sheffield¹, Eric F. Wood¹ & Michael L. Roderick²

Drought is expected to increase in frequency and severity in the future as a result of climate change, mainly as a consequence of decreases in regional precipitation but also because of increasing evaporation driven by global warming^{1–3}. Previous assessments of historic changes in drought over the late twentieth and early twenty-first centuries indicate that this may already be happening globally. In particular, calculations of the Palmer Drought Severity Index (PDSI) show a decrease in moisture globally since the 1970s with a commensurate increase in the area in drought that is attributed, in part, to global warming^{4,5}. The simplicity of the PDSI, which is calculated from a simple water-balance model forced by monthly precipitation and temperature data, makes it an attractive tool in large-scale drought assessments, but may give biased results in the context of climate change⁶. Here we show that the previously reported increase in global drought is overestimated because the PDSI uses a simplified model of potential evaporation⁷ that responds only to changes in temperature and thus responds incorrectly to global warming in recent decades. More realistic calculations, based on the underlying physical principles⁸ that take into account changes in available energy, humidity and wind speed, suggest that there has been little change in drought over the past 60 years. The results have implications for how we interpret the impact of global warming on the hydrological cycle and its extremes, and may help to explain why palaeoclimate drought reconstructions based on tree-ring data diverge from the PDSI-based drought record in recent years^{9,10}.

Drought is a major natural hazard that can have devastating impacts on regional agriculture, water resources and the environment, with far-reaching impacts in an increasingly globalized world¹¹. The perceived abundance of drought in the 2000s, such as long-term events in the western United States, southeast Australia and northeast China, and the recent short-term but severe events in Russia and the central United States, hint that climate change may be a forcing factor and this is only likely to get worse, given projected climate warming and precipitation changes for the twenty-first century^{1,2}. Many studies have attributed the severity and length of recent droughts to global warming^{5,12}. The Fourth Assessment Report (AR4) of the Intergovernmental Panel on Climate Change (IPCC) summarized the evidence in the following terms: “More intense and longer droughts have been observed over wider areas since the 1970s, particularly in the tropics and subtropics. Increased drying linked with higher temperatures and decreased precipitation has contributed to changes in drought”¹³. The AR4 drew heavily from historic analyses of the PDSI, which shows an increase in drought in the last few decades, regionally^{5,14} and globally⁴, that is commensurate with the increase in global temperatures. The AR4 summary has been substantially revised, however, in the recent IPCC Special Report on Extremes³ that notes the over-reliance on the PDSI and possible overestimation of the increase in regional and global drought.

The PDSI was developed originally as an agricultural monitoring tool in the United States in the 1960s¹⁵ that helped in allocating aid to stricken farmers. It is used pervasively for operational monitoring and increasingly in studies of climate change^{2,16}. Its popularity stems from

its ease of use and long history in agricultural applications. However, the PDSI has several shortcomings because of its simplicity^{3,17,18}, including the treatment of potential evaporation (PE, the evaporative demand of the atmosphere), which is calculated from temperature data by using the empirical Thornthwaite equation⁷. It has been well established that evaporation is a function of more than just temperature, and the correct physics includes radiative and aerodynamic controls on evaporative demand^{8,19–21}. Temperature-based PE methods apparently perform relatively well in climatological applications because air temperature is correlated with net radiation and humidity at weekly, monthly and subannual timescales²². However, estimating trends is problematic and there is extensive literature showing that temperature-based methods are flawed, inherently because the temperature state does not uniquely determine the evaporative flux (see Supplementary Information). In the context of climate change, the temperature-based approach responds to recent observed warming with increasing PE. When used in the PDSI model, which derives soil moisture from the balance between precipitation, evaporation and runoff, the increase in PE drives an increase in drought globally¹³ in addition to the impact of any changes in precipitation. However, numerous studies based on observations and detailed physical modelling have shown regional declines in evaporative demand over past decades as a result of various combinations of declining radiation, vapour-pressure deficit and/or wind speed⁶, despite generally increasing regional temperatures.

To resolve this discrepancy and provide an improved estimate of changes in global drought over the past 60 years based on better

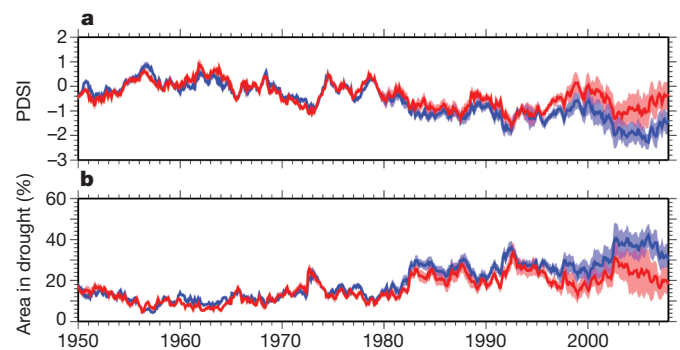


Figure 1 | Global average time series of the PDSI and area in drought. **a**, PDSI_Th (blue line) and PDSI_PM (red line). **b**, Area in drought (PDSI < -3.0) for the PDSI_Th (blue line) and PDSI_PM (red line). The shading represents the range derived from uncertainties in precipitation (PDSI_Th and PDSI_PM) and net radiation (PDSI_PM only). Uncertainty in precipitation is estimated by forcing the PDSI_Th and PDSI_PM by four alternative global precipitation data sets. Uncertainty from net radiation is estimated by forcing the PDSI_PM with a hybrid empirical–satellite data set³¹ and an empirical estimate. The other near-surface meteorological data are from a hybrid reanalysis–observational data set³¹. The thick lines are the mean values of the different PDSI data sets. The time series are averaged over global land areas excluding Greenland, Antarctica and desert regions with a mean annual precipitation of less than 0.5 mm d⁻¹.

¹Department of Civil and Environmental Engineering, Princeton University, Princeton, New Jersey 08544, USA. ²Australian Research Council Centre of Excellence for Climate System Science, Research School of Earth Science & Research School of Biology, The Australian National University, Canberra ACT 0200, Australia.

physics, we calculate global changes in the PDSI using two methods for PE. We use the Thornthwaite algorithm and a physically based estimate based on the currently accepted Penman–Monteith (PM) equation^{19,23} forced by our global meteorological data set and a set of alternative precipitation and net radiation data sets (see Methods). Because the PM is a more accurate, comprehensive and physically based model of PE (see Supplementary Information), it also has greater data requirements, which until recently has precluded its use at large scales. However, the increasing availability of detailed meteorological data from gridded ground observations, satellite remote sensing and atmospheric model reanalyses now makes it possible to calculate improved estimates that take into account radiative and aerodynamic controls. Recent studies have claimed that there is little difference between the PDSIs that use the Thornthwaite and PM algorithms (PDSI_Th and PDSI_PM, respectively)^{24,25} but this can be attributed to inconsistencies in the forcing data sets and simulation configuration (see Supplementary Information).

The global averaged time series of PDSI using the two PE methods (Fig. 1a) clearly shows the decreasing trend in the PDSI_Th since the 1970s but not for the PDSI_PM. Uncertainty due to precipitation and net radiation is estimated using four different global precipitation data sets and two different net radiation data sets, and is represented by the shading. The trend for 1950–2008 is $-0.037 \pm 0.004 \text{ yr}^{-1}$ ($P < 0.01$) and $-0.018 \pm 0.005 \text{ yr}^{-1}$ ($P < 0.01$) for the PDSI_Th and PDSI_PM, respectively. The more recent trend over 1980–2008 is similar for the PDSI_Th ($-0.032 \pm 0.008 \text{ yr}^{-1}$; $P < 0.01$) but is essentially zero for the PDSI_PM ($0.003 \pm 0.018 \text{ yr}^{-1}$; not significant). The global area in

drought (Fig. 1b) from 1980 to 2008 increases by $0.559 \pm 0.117\%$ per year ($P < 0.01$) for the PDSI_Th and increases by $0.078 \pm 0.205\%$ per year (not significant) for the PDSI_PM. Despite the smaller overall trend in PDSI_PM, there is still an increase in drought area, although this is seven times smaller than the PDSI_Th drought area trend. The spatial distribution of trends in the PDSI_Th (Fig. 2) shows drying across much of the global land, particularly over Africa and eastern Asia. In contrast, the PDSI_PM shows a mixture of drying and wetting that combines to give a smaller trend globally. The equivalent trends in the PE_Th are increasing everywhere (98% of land area), as expected given the global increase in temperature, but are a mixture of increases (58% of land area) and decreases (42%) for the PE_PM. The two methods disagree in the sign of the trends across much of northern South America, Central America, eastern North America, eastern sub-Saharan Africa, western Russia, southern and southeast Asia, and Australia. Because some of these regions are water-limited, the impact on actual evaporation, and therefore the PDSI, is small. However, in energy-limited regions such as northern Eurasia and the Amazon, the differences in PE translate into differences in the sign of the PDSI trends.

The results show that previous calculations of the increase in global drought are overestimated. However, there are several sources of uncertainty in our approach, not least from the errors in the meteorological data. We use contemporary data, which are the best that are currently available globally, but we recognize that they are not perfect. Nevertheless, the regions of decreasing PE trends estimated with the PM model are generally in agreement with the abundance of evidence

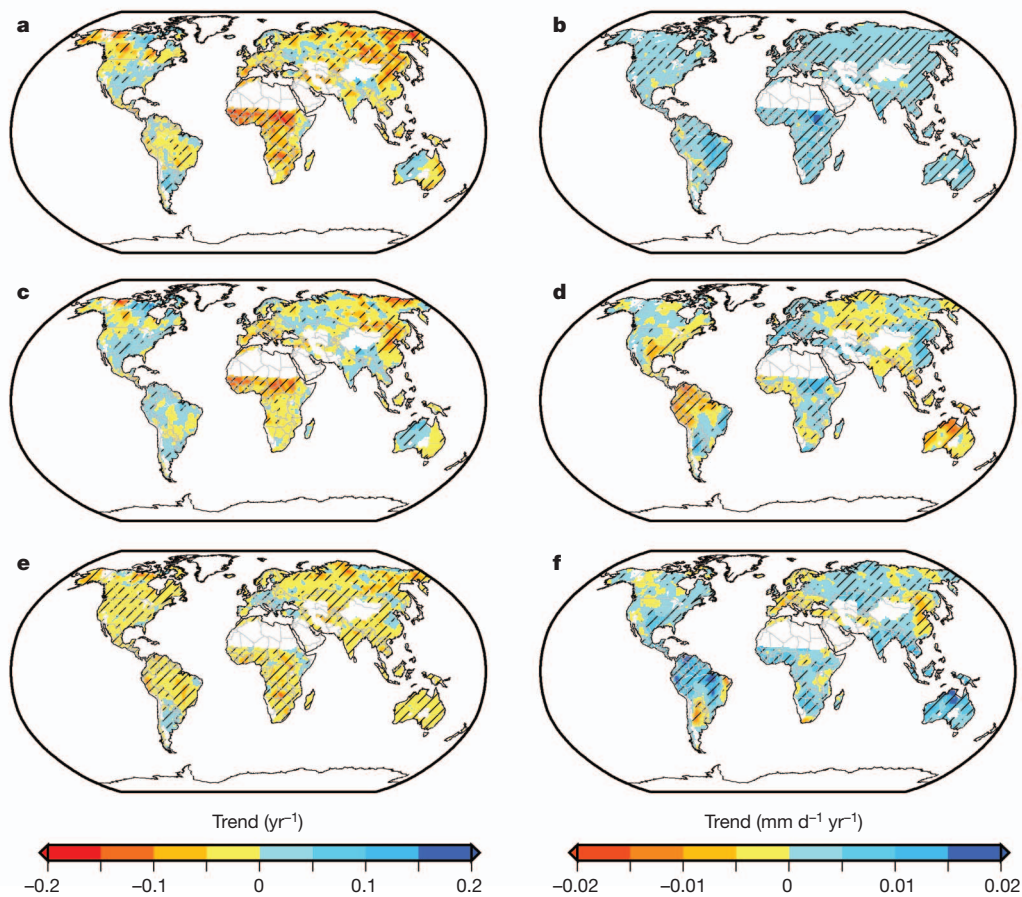


Figure 2 | Trends in the PDSI and PE. a, c, e, Non-parametric trends for 1950–2008 in annual average PDSI (averaged over the results using the four precipitation data sets and, for the PDSI_PM, also over the two net radiation data sets) from the PDSI_Th (a) and the PDSI_PM (c), and their difference (e). b, d, f, Non-parametric trends for 1950–2008 in annual average PE from the Thornthwaite equation

(b) and the PM equations (d), and their difference (f). Values are not shown for Greenland, Antarctica and desert regions with a mean annual precipitation of less than 0.5 mm d^{-1} . Statistically significant trends at the 95% level are indicated by hatching. The difference in trends in e and f and its statistical significance are calculated from the time series of differences between the two data sets.

of decreasing pan evaporation for many regions⁶, which has been attributed to global dimming, decreases in wind speed and in some places decreasing vapour-pressure deficit²⁰ (see Supplementary Information for further discussion). The temperature-based algorithm does not capture these trends. The trends in the radiation, wind-speed and humidity data used to calculate the PE_PM are generally consistent with regional observations, although increasing trends in downward longwave radiation and decreasing trends in wind speed from sparse monitoring networks are generally underestimated by the global data set. However, the possible underestimation of trends in downward longwave radiation cannot explain the difference between the PDSI_Th and PDSI_PM, and underestimation of wind-speed decline implies that the difference is probably a conservative estimate (see Supplementary Information). Furthermore, uncertainty due to the data on precipitation and net radiation as estimated from the standard deviation of PDSI trends for different precipitation and net radiation data sets is much smaller than the difference in PDSI trends due to the PE method. As these data sets improve and the uncertainties are reduced, the magnitude of the calculated trends in drought extent will change; however, the conclusion—that poor physical representation of potential evapotranspiration induces untenable estimates of long-term changes in drought—will remain.

Despite the long-standing consensus that the underlying science for temperature-based estimates of PE is flawed, compounded by the results of this and other studies^{6,21,22} that the flaws are manifested in errors in the estimations of the impact of warming on drought and hydrology in general, the reasons for the long and continued use of the PDSI_Th for climate studies in essentially its original form are a curiosity. The arguments justifying its use are generally based on the availability of data, but they are also probably related to its traditional use for mapping agricultural drought and allocating drought aid, in which comparisons—and thus division of aid—are based on spatial maps made over a short period (weeks to months). Those applications rely on spatial variations that are driven mainly by precipitation deficits, and so the PDSI_Th should do a reasonable job of distinguishing between regions of more or less drought severity at a given instant. However, in the assessment of long-term variations due to climate variability or change, a use for which the PDSI_Th was originally not designed, it seems that the over-sensitivity to changes in temperature, and other simplifications, compromises the comparisons in time. Palaeoclimate reconstructions of drought may be particularly susceptible because they are often developed by scaling tree-ring data to match the calculated PDSI_Th for their overlap period. For some regions, the tree-ring data, which reflect real variations in climatic and non-climatic factors (such as disturbances), diverge from the instrumental-based PDSI_Th in recent decades when warming has been most rapid (see, for example, refs 9, 10). Similarly, the ‘divergence problem’²⁶ as it relates to reconstructions of temperature from high-latitude and high-elevation tree-ring data may be associated with the assumption that temperature can be used as a surrogate for the controls on growth through variations in evapotranspiration, notwithstanding the competing impacts of other environmental factors (for example, higher concentrations of CO₂). This can lead to overestimation of past changes and conversely underestimation of recent trends in the context of the past.

The results of this study have implications for how we interpret the role of global warming in changes to the terrestrial hydrological cycle and its extremes, such as drought, and how we quantify the impacts of future climate change. Several regional studies^{5,12} have suggested that higher temperatures than normal were the cause for increased drought in recent years through increased evaporation. Yet there is evidence that the direct impact of temperature on drying may actually be a misinterpretation of feedbacks between the land and the atmosphere. It is more plausible that evaporation actually decreases during drought²⁷ because of less precipitation, and that drought drives increases in temperatures because there is less evaporative cooling and thus a higher sensible heat flux warming the air²⁸. Short-term temperature anomalies

are likely to be a response to drought, rather than a factor in forcing drought²⁹. Of concern is if the perceived influence of warming on drought as quantified by empirical approaches is extrapolated into the future and predictions of the impacts of climate change are likely to be overestimated^{21,22,30}. It is therefore essential to retain a perspective on the magnitude of impacts of global warming that is based on our physical understanding of the complex relationships between climate and hydrological variability. The use of physically realistic hydrological modelling merged with the wealth of *in situ* and satellite-based data sources has the potential to give better estimates of changes in global drought and its relationship with climate change.

METHODS SUMMARY

We quantify drought with the original and self-calibrating version of the PDSI model¹⁸, which uses the Thornthwaite algorithm (PDSI_Th), and a modified version (PDSI_PM) that uses the PM formulation for PE. The two models (PDSI_Th and PDSI_PM) are forced with precipitation and temperature data from our global meteorological data set³¹, which combines atmospheric reanalysis data with available remote sensing and ground observations and has been updated to 1948–2008. The meteorological data are adjusted to remove spurious trends due to observational system changes (see Supplementary Information). We also use a set of alternative global precipitation data sets to evaluate the impact of uncertainties in global precipitation trends on the drought trends, recognizing that precipitation is the main driver of drought variability but that there are uncertainties in precipitation trends at regional to global scales. The PDSI_PM model additionally requires radiation, humidity and other near-surface meteorological inputs, which are also taken from the updated meteorological data set (see Supplementary Information). Trends in annual mean values are calculated by using the non-parametric Mann–Kendall test and given as the median value across PDSI data sets derived from different precipitation data sets, with the standard deviation given after the \pm sign and estimated by the scaled median absolute deviation. An α value of 0.05 is used to test for significance. The area in drought is calculated as the percentage of land area with a PDSI of less than -3 .

Full Methods and any associated references are available in the online version of the paper.

Received 23 July; accepted 11 September 2012.

1. Sheffield, J. & Wood, E. F. Projected changes in drought occurrence under future global warming from multi-model, multi-scenario, IPCC AR4 simulations. *Clim. Dyn.* **13**, 79–105 (2008).
2. Dai, A. Drought under global warming: a review. *Wiley Interdisc. Rev. Clim. Change* **2**, 45–65 (2010).
3. Seneviratne, S. I. *et al.* in *Managing the Risks of Extreme Events and Disasters to Advance Climate Change Adaptation* (eds Field, C. B. *et al.*) 109–230 (Intergovernmental Panel on Climate Change, 2012).
4. Dai, A., Trenberth, K. E. & Qian, T. A global data set of Palmer Drought Severity Index for 1870–2002: relationship with soil moisture and effects of surface warming. *J. Hydrometeorol.* **5**, 1117–1130 (2004).
5. Briffa, K. R., van der Schrier, G. & Jones, P. D. Wet and dry summers in Europe since 1750: evidence of increasing drought. *Int. J. Climatol.* **29**, 1894–1905 (2009).
6. Roderick, M. L., Hobbins, M. T. & Farquhar, G. D. Pan evaporation trends and the terrestrial water balance II. Energy balance and interpretation. *Geog. Compass* **3**, 761–780 (2009).
7. Thornthwaite, C. W. An approach toward a rational classification of climate. *Geogr. Rev.* **38**, 55–94 (1948).
8. Penman, H. L. Natural evaporation from open water, bare soil, and grass. *Proc. R. Soc. Lond. A* **193**, 120–145 (1948).
9. Fang, K. Y. *et al.* Drought variations in the eastern part of northwest China over the past two centuries: evidence from tree rings. *Clim. Res.* **38**, 129–135 (2009).
10. de Grandpré, L. *et al.* Seasonal shift in the climate responses of *Pinus sibirica*, *Pinus sylvestris*, and *Larix sibirica* trees from semi-arid, north-central Mongolia. *Can. J. For. Res.* **41**, 1242–1255 (2011).
11. Sternberg, T. Regional drought has a global impact. *Nature* **472**, 169 (2011).
12. Cai, W., Cowan, T., Briggs, P. & Raupach, M. Rising temperature depletes soil moisture and exacerbates severe drought conditions across southeast Australia. *Geophys. Res. Lett.* **36**, L21709 (2009).
13. IPCC. *Climate Change 2007: The Physical Science Basis. Contribution of Working Group I to the Fourth Assessment Report of the Intergovernmental Panel on Climate Change* (eds Solomon, S. *et al.*) (Cambridge Univ. Press, 2007).
14. Wang, J., Chen, F., Jin, L. & Bai, H. Characteristics of the dry/wet trend over arid central Asia over the past 100 years. *Clim. Res.* **41**, 51–59 (2010).
15. Palmer, W. C. *Meteorological Drought* (US Department of Commerce Research Paper 45, 1965).
16. Zhao, M. & Running, S. W. Drought-induced reduction in global terrestrial net primary production from 2000 through 2009. *Science* **329**, 940–943 (2010).

17. Alley, W. M. The Palmer Drought Severity Index: limitations and assumptions. *J. Clim. Appl. Meteorol.* **23**, 1100–1109 (1984).
18. Wells, N., Goddard, S. & Hayes, M. J. A self-calibrating Palmer drought severity index. *J. Clim.* **17**, 2335–2351 (2004).
19. Shuttleworth, W. J. in *Handbook of Hydrology* (ed. Maidment, D. R.) 4.1–4.53 (McGraw-Hill, 1993).
20. Roderick, M. L., Rotstayn, L. D., Farquhar, G. D. & Hobbins, M. T. On the attribution of changing pan evaporation. *Geophys. Res. Lett.* **34**, L17403 (2007).
21. Donohue, R. J., McVicar, T. R. & Roderick, M. L. Assessing the ability of potential evaporation formulations to capture the dynamics in evaporative demand within a changing climate. *J. Hydrol. (Amst.)* **386**, 186–197 (2010).
22. Shaw, S. & Riha, S. J. Assessing temperature-based PET equations under a changing climate in temperate, deciduous forests. *Hydrol. Process.* **25**, 1466–1478 (2011).
23. Monteith, J. L. Evaporation and environment. *Symp. Soc. Exp. Biol.* **19**, 205–234 (1964).
24. Dai, A. Characteristics and trends in various forms of the Palmer Drought Severity Index during 1900–2008. *J. Geophys. Res.* **116**, D12115 (2011).
25. van der Schrier, G., Jones, P. D. & Briffa, K. R. The sensitivity of the PDSI to the Thornthwaite and Penman–Monteith parameterizations for potential evapotranspiration. *J. Geophys. Res.* **116**, D03106 (2011).
26. D'Arrigo, R., Wilson, R., Liepert, B. & Cherubini, P. On the 'Divergence Problem' in northern forests: a review of the tree-ring evidence and possible causes. *Global Planet. Change* **60**, 289–305 (2008).
27. Roderick, M. L. & Farquhar, G. D. Changes in Australian pan evaporation from 1970 to 2002. *Int. J. Climatol.* **24**, 1077–1090 (2004).
28. Lockart, N., Kavetski, D. & Franks, S. W. On the recent warming in the Murray–Darling Basin: land surface interactions misunderstood. *Geophys. Res. Lett.* **36**, L24405 (2009).
29. Hirschi, M. *et al.* Observational evidence for soil-moisture impact on hot extremes in southeastern Europe. *Nature Geosci.* **4**, 17–21 (2011).
30. Milly, P. C. D. & Dunne, K. A. On the hydrologic adjustment of climate-model projections: the potential pitfall of potential evapotranspiration. *Earth Interact.* **15**, 1–14 (2011).
31. Sheffield, J., Goteti, G. & Wood, E. F. Development of a 50-yr high-resolution global dataset of meteorological forcings for land surface modeling. *J. Clim.* **19**, 3088–3111 (2006).

Supplementary Information is available in the online version of the paper.

Acknowledgements J.S. acknowledges support from the US National Oceanic and Atmospheric Agency (NA100AR4310130, NA11OAR4310097) and NASA (NNX08AN40A). M.L.R. acknowledges the support of the Australian Research Council (DP0879763, DP110105376, CE11E0098).

Author Contributions J.S. and E.F.W. conceived the study with inspiration from M.L.R. J.S. performed the analyses and mainly wrote the manuscript. E.F.W. and M.L.R. contributed to discussion and the manuscript.

Author Information Reprints and permissions information is available at www.nature.com/reprints. The authors declare no competing financial interests. Readers are welcome to comment on the online version of the paper. Correspondence and requests for materials should be addressed to J.S. (justin@princeton.edu).

METHODS

Palmer Drought Severity Index. Historically, the PDSI¹⁵ has been the tool of choice when monitoring and analysing drought occurrence, especially in the United States, where it is one component of the US National Drought Monitor³². It is generally calculated on weekly to monthly timescales and uses precipitation and temperature inputs to drive a simplified water-balance model with a generic two-layer soil model and meteorology that is normalized with a reference set of water balance terms. At continental to global scales its simplicity makes it an attractive choice for reconstructing drought records^{4,33}, for which it has also been shown to be a proxy for soil moisture⁴. It has been used to analyse continental-scale to global-scale, long-term variability in drought by several studies (see, for example, refs 4, 34, 35). The PDSI is generally well correlated with output from more comprehensive hydrological modelling³⁶ but diverges in cooler seasons and high latitudes, and substantially so in drier regions.

Despite this legacy, the PDSI has been shown to be unsuitable for widespread application and suffers from simplifications in its physical basis and soil hydrology^{17,37}. For example, its exclusion of cold-season processes makes it unsuitable for application in many parts of the world. The usual form of the PDSI algorithm uses several empirical constants to characterize the local climate. These were originally derived by Palmer using data from a number of climate divisions generally located in the midwestern United States and are therefore not representative of the whole globe. For example, the criteria for signalling the start and end of a drought are arbitrarily based on original data from the midwestern United States. Some of the shortcomings have been addressed by a self-calibrating version¹⁸ that removes the spatial inconsistencies.

We quantify drought with the original and self-calibrating version of the PDSI model¹⁸, which uses the Thornthwaite algorithm (PDSI_Th), and a modified version (PDSI_PM) that uses the PM formulation for PE.

Thornthwaite PE algorithm. PE is modelled in the PDSI by using the temperature-only-based Thornthwaite method. Thornthwaite⁷ correlated mean monthly temperature with PE, as determined from the water balance for valleys in the eastern USA, where sufficient moisture was available to maintain active transpiration. The Thornthwaite formula for monthly PE (mm) is

$$PE = 16d(10T/I)^a$$

where T is the mean temperature for the month (in °C) and d is a correction factor that depends on latitude and month. I is the annual thermal index,

$$I = \sum_{i=1}^{12} (T_i/5)^{1.514}$$

where the subscript i refers to the month of the year and a is an empirical factor,

$$a = 0.49 + 0.0179I - 0.0000771I^2 + 0.000000675I^3$$

Penman–Monteith PE algorithm. The PM approach²³ is generally accepted as the most comprehensive algorithm for modelling potential and actual evapotranspiration (given additional estimates of the plant and environmental resistance to atmospheric demand). It is derived from consideration of the equations of the surface energy balance by means of elimination of the surface temperature term. It forms the basis for the evaporation submodel of many distributed hydrological and land surface models, the latter of which often form the land component of coupled climate models, and has been used as the basis for regional and global retrievals of evapotranspiration based on satellite remotely sensed data (see, for example, refs 38–40). The PM equation given below models the diffusion of energy from plants or soil against stomatal and aerodynamic resistance, given inputs of net radiation, temperature, humidity and wind speed:

$$ET = \frac{\Delta R_{\text{net}} + (\rho c_p D / r_a)}{\Delta + \gamma(1 + r_s/r_a)}$$

where evapotranspiration (ET) is now in W m^{-2} , which can be converted into mm per month by dividing by the latent heat of vaporization of water, λ (J kg^{-1}). Δ (Pa K^{-1}) is the slope of the plot of saturated vapour pressure against air temperature, R_{net} is the net radiation (W m^{-2}), ρ is the density of air (kg m^{-3}), c_p is the specific heat of air at constant pressure ($\text{J kg}^{-1} \text{K}^{-1}$), D is the vapour-pressure deficit (Pa) and γ is the psychrometric constant (Pa K^{-1}). r_a and r_s are the aerodynamic and stomatal resistances (s m^{-1}), respectively. ET collapses to PE when the stomatal resistance is zero; the recommended form of the equation¹⁹, given as the sum of the radiative and aerodynamic components, is

$$PE = \frac{\Delta}{\Delta + \gamma} R_{\text{net}} + \frac{\gamma}{\Delta + \gamma} 6.43(1 + 0.536U)D$$

where PE is now in mm d^{-1} ; U is the wind speed (m s^{-1}) at 2 m height. In comparison with the Thornthwaite expression, which is based solely on temperature, the PM models evaporation as the combination of radiative and aerodynamic processes, thus giving a more realistic estimate and having the potential to be influenced by changes in humidity, radiation and wind speed, as well as temperature.

Global meteorological forcing dataset. The two PDSI models (PDSI_Th and PDSI_PM) are forced with precipitation and temperature data from our global meteorological data set. The PDSI_PM model additionally requires radiation, humidity and other near-surface meteorological inputs, which are also taken from this data set. The global meteorological forcing dataset³¹ combines reanalysis data and observations to form a global, long-term (1948–2008), 1.0°, 3-hourly data set of precipitation, surface radiation and near-surface meteorology. The data set is designed for forcing land-surface hydrological models and other physical models at large spatial (regional to global) and temporal (annual to decadal) domains. Thus the goal of the data set is to ensure robustness of long-term trends and variability. At the same time it adjusts the short-term (daily and diurnal) variations to match observational data where available and maintains interrelations between variables. The data set is based on the NCEP/NCAR reanalysis (NNR)⁴¹, which provides continuous records of atmospheric and land variables from 1948 to the present. The reanalysis data are corrected to remove biases at diurnal to annual timescales by merging with observational data for precipitation, air temperature, and shortwave and longwave radiation. Precipitation and temperature are scaled to match the Climatic Research Unit (CRU) TS3.0 data set⁴² on a monthly timescale. The diurnal cycle of precipitation is resampled from a statistical model derived from the Tropical Rainfall Measurement Mission (TRMM) Multi-Satellite Precipitation Analysis (TMPA) satellite-based data set⁴³. The diurnal range in air temperature is also adjusted to match the CRU TS3.0 data set. For 1984–2007, the shortwave and longwave radiation are scaled to match the NASA/GEWEX Surface Radiation Budget (SRB) satellite based data set⁴⁴ on a monthly timescale. The data set is available from <http://hydrology.princeton.edu/data.pgf.php>.

Alternative precipitation data sets. A set of four global precipitation data sets is used to quantify the uncertainty in global precipitation. The data sets are CPC-Prec/L⁴⁵ (<ftp://ftp.cpc.ncep.noaa.gov/precip/50yr/>), Global Precipitation Climatology Centre V4 (ref. 46) (GPCC; <http://gpcc.dwd.de>), Climatic Research Unit TS3.0 (ref. 42) (<http://badc.nerc.ac.uk/browse/badc/cru>) and Willmott–Matsuura V2.01 (ref. 47) (http://climate.geog.udel.edu/~climate/html_pages/download.html).

Trend calculation. Trends in annual mean values are calculated by using the non-parametric Mann–Kendall test and given as the median value across PDSI data sets derived from different precipitation data sets, with the standard deviation given after the \pm sign and estimated by the scaled median absolute deviation. An α value of 0.05 is used to test for significance. The area in drought is calculated as the percentage of land area with a PDSI of less than -3 .

32. Svoboda, M. *et al.* The Drought Monitor. *Bull. Am. Meteorol. Soc.* **83**, 1181–1190 (2002).
33. Cook, E. R., Meko, D. M., Stahle, D. W. & Cleaveland, M. K. Drought reconstructions for the continental United States. *J. Clim.* **12**, 1145–1162 (1999).
34. van der Schrier, G., Briffa, K. R., Osborn, T. J. & Cook, E. R. Summer moisture availability across North America. *J. Geophys. Res.* **111**, D11102 (2006).
35. McCabe, G. J. & Palecki, M. A. Multidecadal climate variability of global lands and oceans. *Int. J. Climatol.* **26**, 849–865 (2006).
36. Sheffield, J. & Wood, E. F. Characteristics of global and regional drought, 1950–2000: analysis of soil moisture data from off-line simulation of the terrestrial hydrologic cycle. *J. Geophys. Res.* **112**, D17115 (2007).
37. Jensen, M. E. *Consumptive Use of Water and Irrigation Water Requirements* (American Society of Civil Engineers, 1973).
38. Mu, Q. *et al.* Development of a global evapotranspiration algorithm based on MODIS and global meteorology data. *J. Geophys. Res.* **112**, G01012 (2007).
39. Cleugh, H. A., Leuning, R., Mu, Q. & Running, S. W. Regional evaporation estimates from flux tower and MODIS satellite data. *Remote Sens. Environ.* **106**, 285–304 (2007).
40. Sheffield, J., Wood, E. F. & Munoz-Arriola, F. Long-term regional estimates of evapotranspiration for Mexico based on downscaled ISCCP data. *J. Hydrometeorol.* **11**, 253–275 (2010).
41. Kalnay, E. *et al.* The NCEP/NCAR 40-Year Reanalysis Project. *Bull. Am. Meteorol. Soc.* **77**, 437–471 (1996).
42. Mitchell, T. D. & Jones, P. D. An improved method of constructing a database of monthly climate observations and associated high-resolution grids. *Int. J. Climatol.* **25**, 693–712 (2005).
43. Huffman, G. J. *et al.* The TRMM Multisatellite Precipitation Analysis (TMPA): Quasi-global, multyear, combined-sensor precipitation estimates at fine scales. *J. Hydrometeorol.* **8**, 38–55 (2007).

44. Gupta, S. K., Stackhouse, P. W., Cox, S. J., Mikovitz, J. C. & Zhang, T. Surface Radiation Budget Project completes 22-year data set. *GEWEX News* **16**, 12–13 (2006).
45. Chen, M., Xie, P., Janowiak, J. E. & Arkin, P. A. Global land precipitation: a 50-yr monthly analysis based on gauge observations. *J. Hydrometeorol.* **3**, 249–266 (2002).
46. Schneider, U., Fuchs, T., Meyer-Christoffer, A. & Rudolf, B. Global precipitation analysis products of the GPCC. *Weather and Climate—Deutscher Wetterdienst—Klimadatenzentrum-WZN* <ftp://ftp-anon.dwd.de/pub/data/gpcc/PDF/GPCC_intro_products_2008.pdf> (2008).
47. Willmott, C. J. & Matsuura, K. Terrestrial Air Temperature: 1900–2008 Gridded Monthly Time Series, version 2.01. *Global Air Temperature Archive* <http://climate.geog.udel.edu/~climate/html_pages/Global2_Ts_2009/README.global_t_ts_2009.html> (2010).